# The surface luminescence of silica nanospheres depending on different excitation wavelengths and accompanied photochemical reactions

**ARTICLE** *in* JOURNAL OF NANOPARTICLE RESEARCH · DECEMBER 2013

Impact Factor: 2.18 · DOI: 10.1007/s11051-013-2113-4



**5 AUTHORS**, INCLUDING:

Lei Yang
Hunan University
**21** PUBLICATIONS **178** CITATIONS

SEE PROFILE

J Nanopart Res (2013) 15:2113
DOI 10.1007/s11051-013-2113-4

RESEARCH PAPER

# The surface luminescence of silica nanospheres depending on different excitation wavelengths and accompanied photochemical reactions

**Lei Yang · Dongpo Su · Yajuan She · Jiazhang Dong · Aiping Hu**

Received: 1 June 2013 / Accepted: 5 November 2013


**Abstract** We report a novel scheme for investigating the emission on the surface of silica depending on different excitation wavelengths and accompanied photochemical reactions. Silica nanospheres with a typical feature of quality fractal are fabricated by drying out the hydrolysates of tetraethylorthosilicate in alcohol-absent aqueous solution. The residual organic groups sustain a comparatively stable surface system, kinetically hindering the relaxation of the defect structures. This surface state provides stable and intermediate energy states to accommodate the excitation electrons. Multiphoton processes accelerate the dissociation energy of the Si–O bond and therefore, greatly decrease the photoreaction threshold of photochemical reactions. Thus, different radiation energy stimulates different photochemical processes and thereby creates different luminescence centers on the surface of silica. It becomes possible to tune the position of the emission band by adjust the excitation conditions. The study is significant not only in control and adjusts the surface defects, but also in color-tunable optoelectronic nanodevice.

**Keywords** Silica · Nanospheres · Photoluminescence · Photochemical reaction

L. Yang (✉) · D. Su · Y. She · J. Dong · A. Hu
College of Materials Science and Engineering, Hunan University, Changsha 410082, People's Republic of China
e-mail: nanoyang@qq.com

## Introduction

The miniaturization down to nanoscale introduces intrinsic peculiar properties, such as the visible photoluminescence under ultraviolet (UV) excitation (Ma et al. 2012; Pizani et al. 2008; Smedskjaer et al. 2011), potentially promising for the use of silica nanoparticles as medical nanoprobes or photoelectronic devices without the need of doping with extrinsic fluorophores (Banerjee et al. 2011; Bonacchi et al. 2011). The photoluminescence of amorphous nanosilica are expected to benefit from plenty of emission-related structure defects (Lavinia et al. 2011). The surface atoms have a different nearest neighbors from that in interior. Therefore, the surface of silica is expected to exhibit peculiar luminescence properties (Vaccaro et al. 2010). Up to now, numerous experimental and theoretical efforts have been devoted on surface defects in crystalline and glassy $SiO_2$ (Lavinia et al. 2011; Vaccaro et al. 2010; Iwasaka et al. 2012; Kong et al. 2010), and a general concept has been concluded that surface defects are generated from the dehydration reaction involved in the condensation of silanol groups (Lavinia et al. 2011; Kong et al. 2010; Atsuko et al. 2007). As the excitation energy is usually below the dissociation energy of the Si–O bond (about 8.26 eV) (Wuu et al. 2005), the role of the photochemical reactions on the generation of luminescence centers has been neglected for a long time. However, as there are a lot of surface states in the nanosized silica, multiphoton process (Reimhult et al.

Published online: 16 November 2013

2002) greatly decreases the photoreaction threshold of photochemical reactions.

In this paper, amorphous silica nanospheres (NSs) have been fabricated by hydrolyzing tetraethylorthosilicate (TEOS) in solution of water and amino acid (Yang and Murase 2010). Organic–inorganic hybrid material is an excellent system to kinetically hinder the relaxation of the defect structures (Green et al. 1997), since the structure defects interact with each other to form more stable but optically inactive siloxane bonds (Atsuko et al. 2007). Both the structure characterization and luminescence properties depending on different excitation wavelengths have been investigated. By analysis the luminescence performance, the luminescence process is confirmed to occur on the surface of silica. The nearest excitation state of $T_1$ (Iwasaka et al. 2012) has attracted special attention. This band is observed neither in excitation spectra nor in optical absorption, though it is indispensable to the visible emissions under the higher energy stimulation in our experiment. This later generated state affirms the productions of new luminescence centers as well as the existence of the photochemical reactions (Lavinia et al. 2011). A new idea is investigated that the surface structure of the amorphous silica changes in the near UV radiation. Multiphoton processes (Reimhult et al. 2002) accelerate the dissociation energy of the Si–O bond and therefore, greatly decrease the photoreaction threshold of photochemical reactions. It is significant to modify the surface structure and surface luminescence properties (Atsuko et al. 2007). The near UV radiation can not only effectively produce strong visible photoluminescence, but also introduce the desirable luminescence centers in silica (Lavinia et al. 2011). The different UV radiation stimulates the different photochemical reactions and thereby creates different luminescence centers on the surface of silica (Green et al. 1997). It is possible, therefore, to control the kinds and amounts of the structure and thereby tunes the luminescence properties by controlling excitation wavelengths.

## Experiment

Based on Stöber method (Yokoi et al. 2009), we developed a simple and general method for the synthesis of silica NSs in aqueous solution. In a typical synthesis, L-lysine (0.06 g, 98 %) was first dissolved in water (70 mL). Then Tetraethoxysilane (3.0 g, 28.0 %, TEOS) was added dropwise into L-lysine solution under constantly magnetic stirring for 21 h. A steady temperature (80 °C) and stirring speed (800 r/min) were maintained throughout the dropping process. The beaker containing above mixture solution (pH $\sim$ 10) was covered by a watchglass kept at 100 °C for 24 h and then uncovered to evaporate the water. Grinding dry remains, nonannealed yellowish powder was obtained. Silica NSs prepared at different hydrolysis temperatures of 60, 80, and 90 °C were labeled as NS1, NS2, and NS3, respectively. Finally, a proportion of NS1, NS2, and NS3 powder was put into a muffle furnace. The furnace temperature was increased to 600 °C and then kept for 6 h. After thermal-treatment, the corresponding was labeled as AS1, AS2, and AS3, respectively. Compared to traditional Stöber method (Yokoi et al. 2009), water is dried up relatively quickly. So many structure defects and organic hybrids are expected to be left on the surface of silica, which will play a vital role on the following photochemical reactions. Compared to high energy radiation (Campbell and Sauer 2013), this defect-introducing method is very simple and convenient.

The as-grown sample was examined by small angle X-ray scatteerring (SAXS) measurements on D/Max 2500 diffractometer with Cu K$\alpha$ irradiation. The X-ray source was operated at 40 kV and 40 mA. The morphology of the as-synthesized sample was obtained by transmission electron microscopy (TEM, JEM-3010) and scanning electron microscopy (SEM, JSM-6700F). The thermogravimetric analysis was conducted on NETZSCH STA 409 PC/PG. Fourier transform infrared (FT-IR) spectra was measured by WQF-410. The absorption spectrum was carried out with a UV-2550 series UV–Vis spectrophotometer. Room temperature PL was taken on a Hitachi F-4500 FL spectrophotometer with a Xe lamp as the excitation light source.

## Results and discussion

The typical SEM and TEM of annealed silica NSs of AS1 are shown in Fig. 1a, b, respectively. The typical TEM of nonannealed silica NSs of NS1 are also shown in Fig. 1c. NSs with a uniform size of 9–15 nm are arranged in a loose arrangement structure. Due to

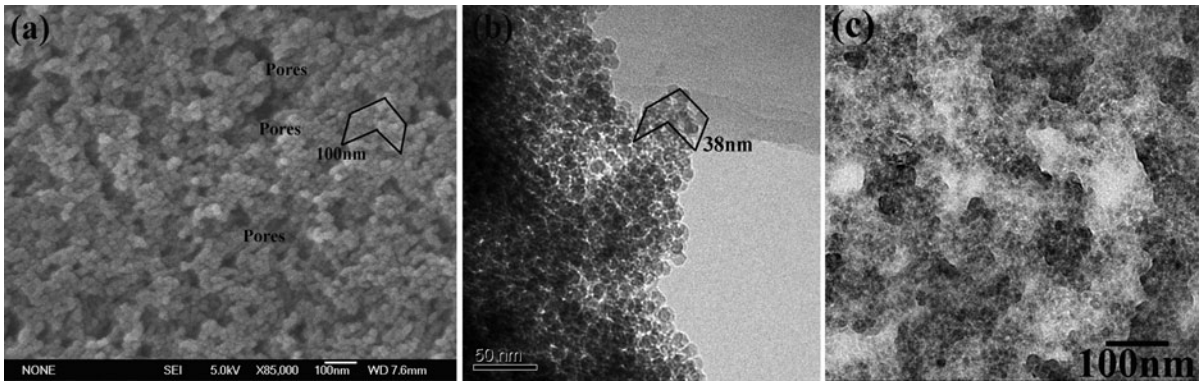


**Fig. 1** The typical SEM image of AS1 and the typical TEM images of AS1 (**b**) and NS1 (**c**)

effect of organic materials, the image of nonannealed silica is not as clear as the annealed one. The SAXS patterns as the function of the interplanar spacing are shown in Fig. 2a. Two obvious plateaus appearing at about 6.39–7.74 and 9.18–11.31 nm, implying there is a certain long-period regular structure. The right shift of the plateaus peak with increase of the hydrolysis temperature provides a pronounced evidence for the increase of the particle size. Due to no sharp peak is found in SAXS curves, the silica particles arrange to regular structure only in a short range, inevitably creating a great of pores in silica. This porous structure is suitable not only for the preservation of the surface hydroxyl groups, but also to effectively absorb the radiation energy. To further characterize the structure of the samples, the relationship of the measured electronic scattering intensity $I_m$ and the scattering vector $q$ are shown in Fig. 2b. They obey with a power function in the high $q$ range:

$$I_m(q) = Aq^{-\alpha} \quad (1)$$

in which $A$ and $\alpha$ are constant. It indicates that the particle density $\rho$ can be described as the power function of distance (Guinier and Fournet 1955; Mo et al. 2010):

$$\rho = Br^{\alpha-3} \quad (2)$$

By linear fitting relationship of $I_m$ and $q$ in double logarithmic coordinate, the value of $\alpha$ is achieved. Thus, the calculated $\alpha - 3$ is $-0.03$, $-0.19$, and $-0.56$ for the samples NS1, NS2, and NS3, respectively. The negative exponent relationship indicates that the organic–inorganic nanocomposite material has a typical feature of quality fractals, a kind of density decreases from particle core to surface (Guinier and Fournet 1955; Mo et al. 2010). It agrees with the previous report that each particle comprises a loose surface shell characterized by a highly disorderly network structure (Vaccaro et al. 2010). Organic groups contribute to sustain a comparatively stable surface system which can kinetically hinder the relaxation of the defect structures. With the increase of hydrolysis temperature, the surface density decreases.

The FTIR spectra of silica particles before and after heat treatment are shown in Fig. 3a. Two hydrogen-related band and three principal SiO absorption bands (Tsu et al. 1989; Umezu et al. 2004) are observed. The absorption peak at 3,452 $cm^{-1}$ and the small peak at 1,640 $cm^{-1}$ represent the OH stretching and bending vibrations of absorbed water on the surface of NSs, respectively (Kim and Kang 2012; Metin et al. 2011). The broad absorption peak indicates that there is a strong interaction between hydroxyls. After heat treatment, the hydroxyl-related absorption peak decreases significantly. The SiO bands at 1,102–1,110, 798–803, and 462–472 $cm^{-1}$ correspond to the stretching, bending, and rocking vibration bands (Lucovsky et al. 1983a, b), respectively. Among them, the stretching band is sensitive to the value of the O/Si ratio and has been used to determine the composition of oxides (Lucovsky et al. 1983a, b; Pai et al. 1986). When the Gaussian multi-peak fitting is applied (shown in Fig. 3b, one weak Si–OH vibration peak (Villegas and Navarro 1988) and two LO–TO splitting peaks (splitting between transverse optical phonon and longitudinal optical phonon) (Leiemann et al. 1984) are observed. The shifts of the TO vibration peak can be approximated with the help of

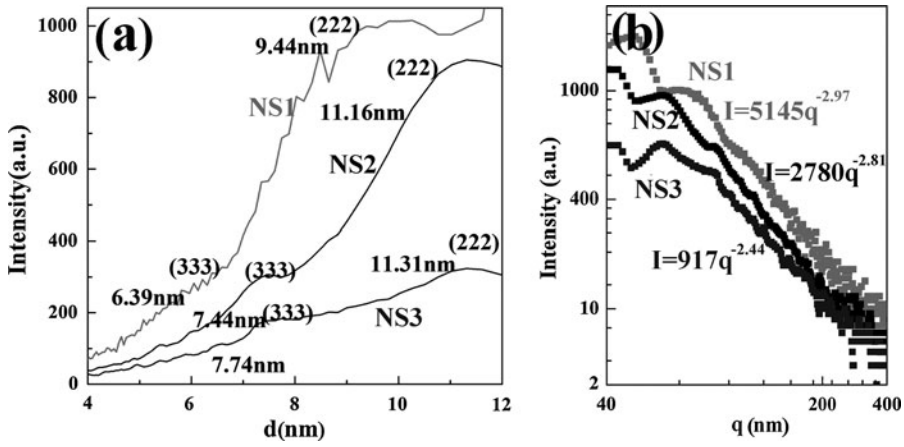


**Fig. 2** The room temperature SAXS patterns of NS1, NS2, and NS3. **a** The measured SAXS patterns as the function of the interplanar spacing *d*. **b** The relationship between the electronic scattering intensity and the modulus of the scattering vector

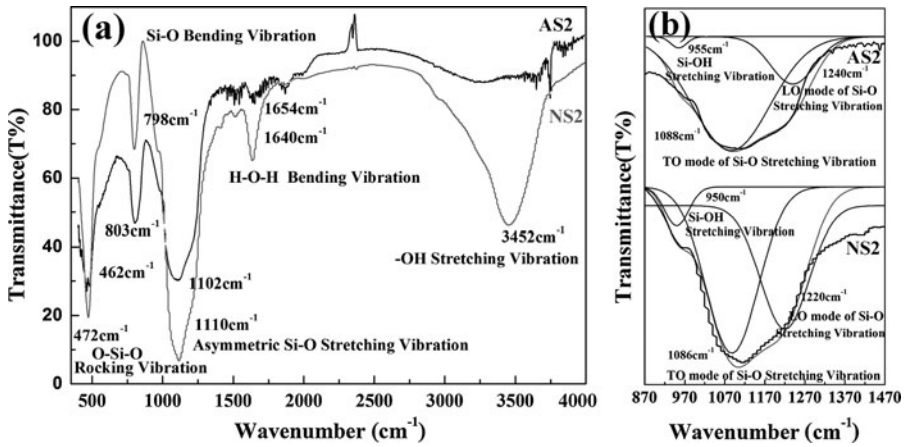


**Fig. 3** The FTIR spectra of the as-prepared samples before and after heat-treated. **a** The typical FTIR spectra in the wavelength range of 350–4,000 $cm^{-1}$. **b** The Gaussian multi-peak fitting for Si–O stretching absorption band, the *black line* represents measured data

simple linear functions of $x$. Therefore, the resulting system

$$v^{R} = 48.8x + 987\left(\mathrm{cm}^{-1}\right) \quad (3)$$

offers a useful method for the determination of the average chemical composition of corresponding $SiO_x$ particles (Schtjmann et al. 1982).

Excess oxygen is found in our sample (O/Si = 2.04 for nonannealed sample and O/Si = 2.07 for annealed sample) under the assumption that the above relationship can be applied to the present silica particles as well. The observed low wavenumber shift $\Delta v$ (2 $cm^{-1}$ in TO phonons) can be interpreted in terms of a decrease in $x$. As far as the silica nanoparticles are concerned, it would be reasonable to deduce that these nanoparticles are chemically oxidized after the heat treatment. The LO mode of SiO stretching vibration absorption peak also shifts to higher frequency ($\Delta v = 20$ $cm^{-1}$) after thermal treatment. It indicates that more SiO bonds are added to the existing oxides (Tian et al. 2010). The FTIR spectra demonstrate that the sample without thermal treatment contains excess oxygen and a lot of surface hydroxyl groups. After thermal treatment, the surface hydroxyl groups decrease greatly, accompanied by the growth of the SiO network.

## The tunable luminescence properties depending on different excitation wavelengths and structural origination

Figure 4 shows the contour maps of three-dimensional fluorescence spectra of silica particle. The PL spectra of the annealed and nonannealed samples at different hydrolysis temperature were measured. It can be seen that except series of multiple-ordered ($\lambda_{em} = n\lambda_{ex}$) scattering peaks, the contour maps of the samples before and after thermal-treatment are quite different. The sample without thermal treatment exhibits two strong luminescence peaks (peak A and B) and one

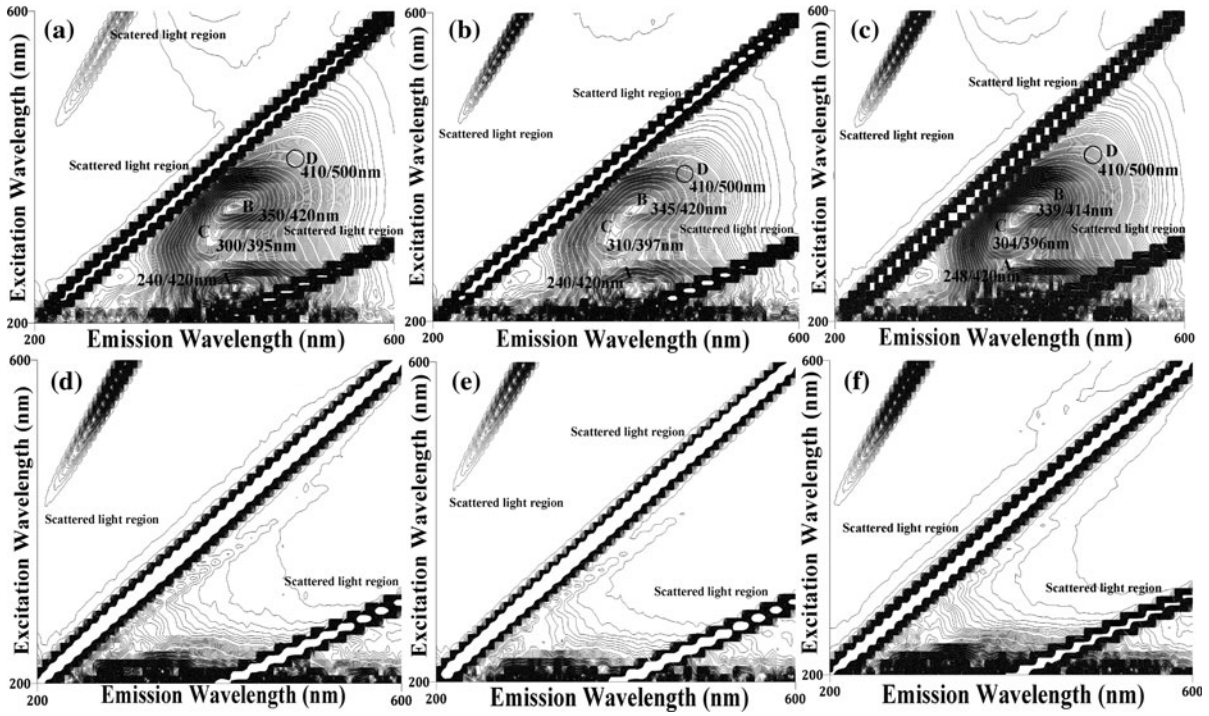


**Fig. 4** The contour maps of three-dimensional fluorescence spectra of **a** NS1, **b** NS2, **c** NS3, **d** AS1, **e** AS2, **f** AS3

luminescence shoulder (peak C). It indicates that there are at least 4 excited states situated at about 2.95 eV (420 nm), 3.14 eV (395 nm), 3.54 eV (350 nm), and 4.13 eV (300 nm) above the ground band. These excited states extend a few tenths of electron volts in the energy band gap to form several excitation bands. While the preparation temperature has only little effect on the location of these luminescence peaks, the thermal treatment exert great influence on the luminescence properties. After thermal treatment, the intensity of luminescence peaks declined considerably. It indicates that the surface hydroxyl groups exert great influence on the luminescent properties of silica.

Figure 5a shows the tunable emission spectra of NS1, NS2, and NS3 at different excitation wavelength. The broad peak at about 420 nm is basically independent of the excitation wavelength as long as an excitation wavelength shorter than 240 nm is employed. Significant enhancement of the 382 and 440–460 nm shoulder is observed with the increase of excitation wavelength from 250 to 310 nm, pushing blue shifts of the emission band. Further increases the excitation wavelength in the range of 320–390 nm, the blue peak shifts to longer wavelength direction. Finally, increase of the excitation wavelength from 400 to 450 nm, the intensity of the emission band decreases greatly. In order to investigate the nonradiation relaxation and the accompanied photochemical reaction, the accurate identification of the emission band is necessary. Both the band spectral position and full with at half-maximum (FWHM) are the criterions. According to the published literature, the emission band at about 420 nm (2.95 eV) with FWHM about 1 eV arises from the surface of dioxasilyrane, $=Si(O_2)$ (Skuja 1998; Boffelli et al. 2013). It indicates that the luminescence occurs on the surface of silica. The narrower emission bands at about 382 nm (3.25 eV) and 440–460 nm (2.70–2.8 eV) arise from the specific structure of silanone (=Si:) (Skuja 1998; Boffelli et al. 2013) and neutral oxygen vacancy (ODCI; $\equiv Si–Si \equiv$) (Skuja 1998; Boffelli et al. 2013), respectively.

The excitation spectra of the NS1, NS2, and NS3, at different monitor wavelength are shown in Fig. 5b. In each excitation, three broad bands at about 224–276 nm (4.49–5.36 eV), 315–380 nm (3.26–3.94 eV), and a weak band at about 278–315 nm (3.94–4.46 eV) are observed. When monitored at 380 nm, the excitation spectra are a little different. The excitation band at about 278–315 nm (3.26–4.46 eV) become strong. These

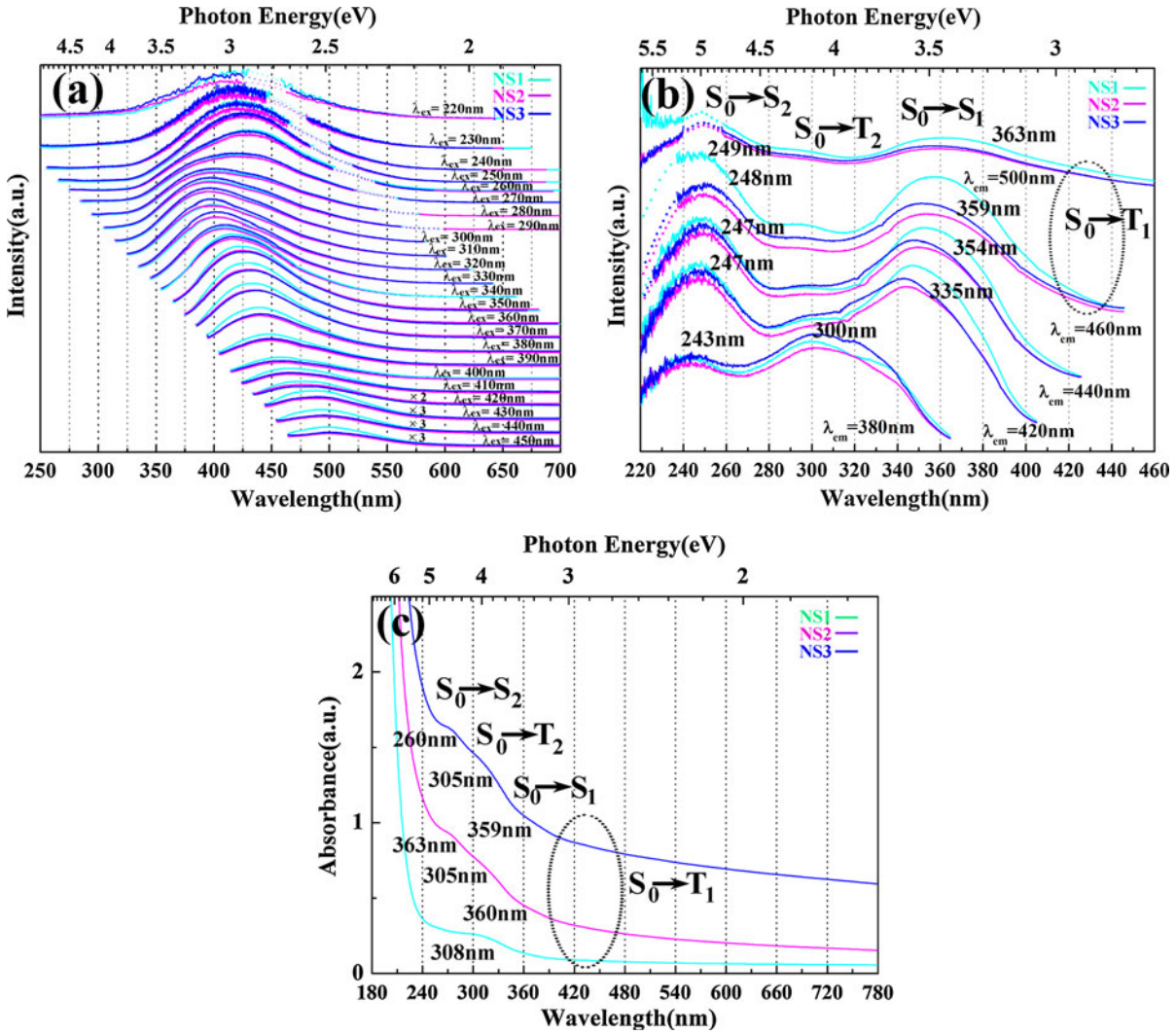


**Fig. 5** The excitation spectra (**a**) at the different excitation wavelength, the tunable emission spectra (**b**) at the different monitor wavelength, and the UV–Vis optical absorption (**c**) of NS1 (*cyan*), NS2 (*magenta*) and NS3 (*blue*). Four emission curves have been amplified. (Color figure online)

excitation bands cannot originate from silanone defect center, the $T_1$, $S_1$, and $S_2$ band of which is located at 3.3, 5.0, and 7.4 eV above the ground state (Iwasaka et al. 2012; Chiodini et al. 2000; Cannas et al. 1997). They cannot originate from ODCI defect center either (Boffelli et al. 2013). On the basis of high-level ab abinitio quantum chemical calculation on the clusters on the surface of silica 9 (Krishnan and Gianfranco 2001), the position of the luminescence bands is in quite good agreement with the $S_0 \rightarrow S_2$, $S_0 \rightarrow T_2$, and $S_0 \rightarrow S_1$ transition of surface dioxasilyrane clusters—$(HO)_2Si(O_2)$. In consideration that a large number of surface hydroxyl groups found in our sample, the excitation bands can be ascribed to the absorption of the whole surface system mainly made up of hydroxyl groups, $=Si(OH)_2$. Here it should also be remarked the controversial the region around 4.49–5.36 and 3.26–3.94 eV: two surface defects, silanone and dioxasilyrane, are thought to have excitaion bands at this energy. It implies that there are a small number of silanones and dioxasilyranes on the surface of silica. The number of dioxasilyranes should be more than that of silanones for the excess oxygen is found. The strong excitation bands provide firm evidence that the surface

system can provide a stable intermediate state to accommodate the excitation electrons.

Figure 5c shows the optical absorption of NS1, NS2, and NS3, in which a strong absorption edge (at about 220 nm, 5.64 eV) and an absorption shoulder band (at about 275–308 nm, 4.51–4.03 eV) are observed. By careful observation, three subbands have been found. These subbands can be assigned to the absorption transitions of $S_0 \rightarrow S_2$, $S_0 \rightarrow T_2$, and $S_0 \rightarrow S_1$ on the surface of silica, respectively. Comparing the optical absorption with the excitation spectra, more details have been found. Although the strong surface $S_1$ band is observed in the excitation spectra, it becomes quite weak in the optical absorption. It illustrates that the $S_1$ band is an unstable state. In addition, none of the $T_1$ bands of the luminescence centers (silanones, surface dioxasilyranes and ODCIs) is observed in excitation spectra or optical absorption, though it is indispensable to the visible emissions. It provides convincing evidence that most of these three structure defects are created after UV radiation. Therefore, the excitation in the range of 400–420 nm cannot produce any strong visible emissions.

Since the excitation transition and the emission transition attribute to the different luminescence centers, electron and energy transfer processes inevitably occurs in the nonradioactive relaxation. When an excitation wavelength of 220–240 nm (5.17–5.64 eV) is employ, the system is promoted from $S_0$ to the excitation state of surface $S_2$. The observed 420 nm emission illustrates that the relaxation of Surface $S_2 \rightarrow$ Dioxasilyranes $T_1$ has occurred. As the $T_1$ band of dioxasilyranes is not found, most of these defects are created after excitation. Similar to the condensation reaction of silanol groups (Nishimura et al. 2009), the photochemical reaction involves the following two reactions:

$$=\mathrm{Si(OH)_2} + =\mathrm{Si(OH)_2} + h\nu \rightarrow =\mathrm{Si}: + =\mathrm{Si(O_2)} + 2\mathrm{H_2O}$$

$$=\mathrm{Si}: + =\mathrm{Si}: \rightarrow =\mathrm{Si}—\mathrm{Si}=$$

The dehydroxylation reaction needs to overcome a potential barrier, about 10.6 eV to break H–O bond (Belau et al. 2007). Since the Surface $S_2$ band is about 4.49–5.36 eV above the ground state, the excitation energy of 5.17–5.64 eV can break the H–O bond at this state. The same position of the $S_2$ excitation band for silanones and dioxasilyranes can be explained in terms of above photochemical reactions.

The relaxation of Surface $T_2 \rightarrow$ Silanone $T_1$ is found after electrons excitated to the surface $T_2$ band, while the 260–310 nm (4.00–4.77 eV) excitation wavelengths are employed. This relaxation process involved another photochemical reaction:

$$=\mathrm{Si(O_2)} + h\nu \rightarrow =\mathrm{Si}: + \mathrm{O_2}$$

The excitation energy in this range can just break the Si–O bond (about 8.26 eV) (Wuu et al. 2005) with the participation of phonons. So, the red shift of the emission band is observed. By analysis the position of lowest absorption band, the threshold energy of dehydroxylation reaction is determined at about 3.77 eV.

The radiation of 340–390 nm (3.18–3.65 eV) stimulates the electrons to the surface state of $S_1$, followed by the relaxation of Surface $S_1 \rightarrow$ ODCI $T_1$. The absence of $T_1$ band indicates the generation process of ODCI defects. It involves interconversions between silanones and ODCIs (Skuja 1998):

$$=\mathrm{Si}: + h\nu \rightarrow =\mathrm{Si}^+ + e^-$$

$$=\mathrm{Si}^+ + =\mathrm{Si}= \rightarrow \equiv \mathrm{Si} - \mathrm{Si} \equiv + =\mathrm{Si}=$$

As this luminescence centers are created in the photochemical reaction, further decrease the excitation energy cannot promote the electrons to the lower $T_1$ band. Therefore, only the weak emissions have been found.

## Conclusion

Amorphous silica NSs with the uniform diameter of 9–15 nm have been synthesized by hydrolyzing TEOS in solution of water and amino acid. These NSs with a typical feature of quality fractal sustain a comparatively stable surface system, kinetically hindering the relaxation of the defect structures. A lot of surface hydroxyl groups and excess oxygen are found in the nonannealed samples. The surface hydroxyl groups exert great influence on the luminescent behavior of silica. After thermal treatment, the surface hydroxyl groups decrease greatly, accompanied by the slight oxidation and growth of the silica clusters.

The surface system mainly made up of hydroxyl groups provides stable and intermediate energy states to accommodate the excitation electrons. The existence of these surface states reduces the reaction

barrier of photochemical reactions. Different radiation energy stimulates different photochemical processes: an excitation wavelength of 220–370 nm stimulates surface dehydroxylation reaction, while the radiation in the range of 340–380 nm promotes the interconversions between silanones and ODCIs. As different defect states are generated by different photochemical process, the position of the emission band can be effectively tuned. With increase of excitation wavelength, a generally red shift of emission band is found, except the appearance of the abnormal blue shift under the excitation in the range of 270–320 nm. It is because the excitation energy in this range stimulates the deoxygenation reactions of dioxasilyranes.

**Acknowledgments** This work was supported by the National Natural Science Foundation of China (Grant No. 11104066), Hunan Provincial Natural Science Foundation of China (Grant No. 2013JJ8004), the Fundamental Research Funds for the Central Universities (Grant No. 531107040172) and China Scholarship Council (No. 201208430255).

## References

Atsuko A, Naoko K, Tomoko Y (2007) Influence of thermal treatments on the photoluminescence characteristics of nanometer-sized amorphous silica particles. J Phys Chem C 111(24):8483–8488

Banerjee S, Honkote S, Datta A (2011) Interaction of surface trap states and defect pair of photoluminescent silica nanostructures with $H_2O_2$ and solvents. J Phys Chem C 115(5):1576–1581

Belau L, Wilson KR, Leone SR, Ahmed M (2007) Vacuum ultraviolet (VUV) photoionization of small water clusters. J Phys Chem A 111(42):10075–10081

Boffelli M, Back M, Cattaruzza E, Gonella F, Trave E, Leto A, Glisenti A, Pezzotti G (2013) Off-stoichiometry spectroscopic investigations of pure amorphous silica and N-doped silica thin films. J Phys Chem C 117(7):3475–3482

Bonacchi S, Genovese D, Juris R, Montalti M, Prodi L, Rampazzo E, Zaccheroni N (2011) Luminescent silica nanoparticles: extending the frontiers of brightness. Angew Chem Int Ed 50(18):4056–4066

Campbell CT, Sauer J (2013) Introduction: surface chemistry of oxides. Chem Rev 113(6):3859–3862

Cannas M, Boscaino R, Gelardi FM, Leone M (1997) Stationary and time dependent PL emission of v-$SiO_2$ in the UV range. J Non-Cryst Solids 216(1–3):99–104

Chiodini N, Meinardi F, Morazzotti F, Paleari A, Scotti R, Martino DD (2000) Photoluminescence of Sn-doped $SiO_2$ excited by synchrotron radiation. J Non-Cryst Solids 261(1–3):1–8

Green WH, Le KP, Grey J, Au TT, Sailor MJ (1997) White phosphors from a silicate–carboxylate sol–gel precursor that lack metal activator ions. Science 276(5320):1826–1828

Guinier A, Fournet G (1955) Small-angle scattering of X-rays. Wiley, New York

Iwasaka T, Inoue K, Katayama R, Uchino T (2012) Synthesis of luminescent silica crystals via a sonochemical reduction route. J Phys Chem C 116(11):6754–6761

Kim BJ, Kang KS (2012) Fabrication of a crack-free large area photonic crystal with colloidal silica spheres modified with vinyltriethoxysilane. Cryst Growth Des 12(8):4039–4042

Kong D, Zhang CM, Xu ZH, Li GG, Hou ZY, Lin J (2010) Tunable photoluminescence in monodisperse silica spheres. J Colloid Interface Sci 352(2):278–284

Krishnan R, Gianfranco P (2001) Photoabsorption of dioxasilyrane and silanone groups at the surface of silica. J Chem Phys 114(10):4657–4663

Lavinia V, Adriana M, Viktor R, Marco C (2011) Bright visible luminescence in silica nanoparticles. J Phys Chem C 115(40):19476–19481

Leiemann A, Sciiuxilyn L, Hübner K (1984) Optical phonons in amorphous silicon oxides. II. Calculation of phonon spectra and interpretation of the IR transmission of $SiO_x$. Phys Stat Sol (b) 121(2):505–511

Lucovsky G, Wong CK, Pollard WB (1983a) Vibrational properties of glasses: intermediate range order. J Non-Cryst Solids 50–60(2):839–846

Lucovsky G, Yang J, Chao SS, Tyler JE, Czubatyj W (1983b) Oxygen-bonding environments in glow-discharge-deposited amorphous silicon–hydrogen alloy films. Phys Rev B 28(6):3225–3233

Ma K, Sai H, Wiesner U (2012) Ultrasmall sub-10 nm near-infrared fluorescent mesoporous silica nanoparticles. J Am Chem Soc 134(32):13180–13183

Metin CO, Lake LW, Miranda CR, Nguyen QP (2011) Stability of aqueous silica nanoparticle dispersions. J Nanopart Res 13(2):839–850

Mo ZS, Zhang ZS, Zhang JD (2010) Structure of crystalline polymers by X-ray diffraction. Science Press, Changchun

Nishimura A, Sagawa N, Uchino T (2009) Structural origin of visible luminescence from silica based organic—inorganic hybrid materials. J Phys Chem C 113:4260–4262

Pai PG, Chao SS, Takagi Y, Lucovsky G (1986) Infrared spectroscopic study of SiOx films produced by plasma enhanced chemical vapor deposition. J Vac Sci Technol A 4(3):689–694

Pizani PS, Joya MR, Pontes FM, Santos LPS, Godinho M Jr, Leite ER, Longo E (2008) Tunable visible photoluminescence of powdered silica glass. J Non-Cryst Solids 354(2–9):476–479

Reimhult E, Höök F, Kasemo B (2002) Vesicle adsorption on $SiO_2$ and $TiO_2$: dependence on vesicle size. J Chem Phys 117(16):7401–7404

Schtjmann L, Lehmann A, Sobotta H, Riede V, Teschner U, Hubner K (1982) Infrared studies of reactively sputtered $SiO_x$ films in the composition range $0.2 \leqq x \leqq 1.9$. Phys Stat Sol (b) 110(1):K69–K73

Skuja L (1998) Optically active oxygen-deficiency-related centers in amorphous silicon dioxide. J Non-Cryst Solids 239(1–3):16–48

Smedskjaer MM, Wang J, Yue YZ (2011) Tunable photoluminescence induced by thermal reduction in rare earth doped glasses. J Mater Chem 21(18):6614–6620

Tian R, Seitz O, Li M, Hu WC, Chabal YJ, Gao JM (2010) Infrared characterization of interfacial Si–O bond formation on silanized flat $SiO_2$/Si surfaces. Langmuir 26(7): 4563–4566

Tsu DV, Lucovsky G, Davidson BN (1989) Effects of the nearest neighbors and the alloy matrix on SiH stretching vibrations in the amorphous $SiO_r$:H ($0 < r < 2$) alloy system. Phys Rev B 40(3):1795–1805

Umezu I, Matsumoto K, Inada M, Makino T, Sugimura A (2004) Correlation between surface oxide and photoluminescence properties of Si nanoparticles prepared by pulsed laser ablation. Appl Phys A 79(4–6):1545–1547

Vaccaro G, Agnello S, Buscarino G, Gelardi FM (2010) Thermally induced structural modification of silica nanoparticles investigated by Raman and infrared absorption spectroscopies. J Phys Chem C 114(33):13991–13997

Villegas MA, Navarro JMF (1988) Characterization of BaOa–SiOa glasses prepared via sol–gel. J Mater Sci 23(7):2464–2478

Wuu DS, Lo WC, Chiang CC, Lin HB, Chang LS, Horng RH, Huang CL, Gao YJ (2005) Water and oxygen permeation of silicon nitride films prepared by plasma enhanced chemical vapor deposition. Surf Coat Technol 198(1–3):114–117

Yang P, Murase N (2010) Preparation-condition dependence of hybrid $SiO_2$-coated CdTe nanocrystals with intense and tunable photoluminescence. Adv Funct Mater 20(8): 1258–1265

Yokoi TJ, Wakabayashi Y, Otsuka W, Fan M, Iwama R, Watanabe K, Aramaki A, Shimojima T Tatsumi, Okubo T (2009) Mechanism of formation of uniform-sized silica nanospheres catalyzed by basic amino acids. Chem Mater 21:3719–3729